

13 **Abstract**

14 The phenomenon of adsorption is widely exploited across a range of industries to remove
15 contaminants from gases and liquids. Much recent research has focused on identifying low-
16 cost adsorbents which have the potential to be used as alternatives to expensive industry
17 standards like activated carbons. Evaluating these emerging adsorbents entails a considerable
18 amount of labor intensive and costly testing and analysis. This study proposes a simple, low-
19 cost method to rapidly assess the potential of novel media for potential use in large-scale
20 adsorption filters. The filter media investigated in this study were low-cost adsorbents which
21 have been found to be capable of removing dissolved phosphorus from solution, namely: i)
22 aluminum drinking water treatment residual, and ii) crushed concrete. Data collected from
23 multiple small-scale column tests was used to construct a model capable of describing and
24 predicting the progression of adsorbent saturation and the associated effluent concentration
25 breakthrough curves. This model was used to predict the performance of long-term, large-
26 scale filter columns packed with the same media. The approach proved highly successful, and
27 just 24-36 hours of experimental data from the small-scale column experiments was found to
28 provide sufficient information to predict the performance of the large-scale filters for up to
29 three months.

30 **Keywords:** Low-cost adsorbents, adsorption, phosphorus, wastewater treatment

31 Nomenclature

a	Time constant in Eqn. 6/Eqn.13
a*	Time constant in Eqn. 7/Eqn.14
a**	Time constant in Eqn. 8/Eqn.15
A	Constant of proportionality in Eqn. 12 (mg g^{-1})
B	Constant of system heterogeneity in Eqn. 12
C	Sorbate concentration in bulk solution (mg L^{-1})
C _b	Breakthrough concentration (mg L^{-1})
C _e	Sorbate concentration of filter effluent (mg L^{-1})
C _o	Sorbate concentration of filter influent (mg L^{-1})
k _{BA}	Bohart-Adams rate constant ($\text{L mg}^{-1} \text{min}^{-1}$)
M	Mass of adsorbent (g)
N	Residual sorption capacity of bed (mg L^{-1})
N'	Fractional residual sorption capacity (N/N_o)
N _o	Sorption capacity of bed at equilibrium (mg L^{-1})
N _t	Time dependent sorption capacity of bed (mg L^{-1})
Q	Filter loading rate (L min^{-1})
q _e	Equilibrium sorbate concentration per unit mass of adsorbent (mg g^{-1})
q _t	Time dependent sorbate concentration per unit mass of adsorbent (mg g^{-1})
t	Service time/operating time of bed (min)
t _b	Service time/operating time of bed at breakthrough (i.e. when $C_e = C_b$) (min)
U	Flow velocity of solution past adsorbent (cm min^{-1})
V	Volume of solution filtered (L)
V _B	Empty bed volumes of solution filtered
V _x	Filter-bed volume to a bed depth of 'x'(L)
Z	Filter bed depth (cm)

32 **1. Introduction**

33 Adsorbents are used to remove contaminants from gases and liquids across a diverse range of
34 industries including manufacturing, agriculture, mining, and the treatment of both drinking
35 water and municipal wastewater (Dąbrowski, 2001). These industries are naturally interested
36 achieving optimum treatment efficiency with minimal investment, and there has been a
37 growing interest in 'low-cost adsorbents', which are emerging as alternatives to more
38 expensive and well-established adsorbents such as activated carbons (Babel and Kurniawan,
39 2003; Crini, 2006). The term 'low-cost adsorbent' can be used to describe any abundantly
40 available natural material, industrial byproduct, or waste material which, with minimal
41 processing, has suitable physical and chemical properties to allow for its use in the adsorption
42 of some contaminant of interest (Bailey et al., 1999). Such media often display lower
43 adsorption affinities and saturation capacities than well-established adsorbents, like activated
44 carbons and synthetic resins, but they can nonetheless replace these ostensibly 'better' media
45 with the introduction of minor modifications to adsorption treatment processes (Brown et al.,
46 2000; Reddad et al., 2002) - for example, increasing the hydraulic residence time of a filter
47 bed or increasing the adsorbent dose in a batch reactor. Therefore, despite the fact that low-
48 cost adsorbents often display less favorable adsorption characteristics, their use is nonetheless
49 a highly attractive option because of their ability to ultimately achieve equal treatment
50 efficacy to established adsorbents, but at a greatly reduced cost.

51 The interaction between an adsorbent material and a dissolved contaminant is a highly
52 complex one, influenced by a multitude of factors such as the physicochemical properties of
53 the adsorbent and target adsorbate (Bockris et al., 1995), the composition and pH of the
54 solution matrix (Faust and Aly, 1998), and the contact mechanism (i.e. batch or through-
55 flow) between adsorbent and adsorbate (Goel et al., 2005). The complexity of these

56 interactions makes characterizing the adsorptive properties of a medium for a given
57 contaminant a vital first step in assessing its suitability for any intended treatment process. As
58 low-cost adsorbents are often derived from locally sourced natural materials, industrial by-
59 products, and waste materials, there is an inherent variability in their physical structure and
60 chemical composition; no two low-cost adsorbents are exactly alike, and consequently, no
61 two adsorbents will display identical adsorption characteristics. This problem is exacerbated
62 by the fact that there is equal variability in waste streams, and hence there results an
63 unavoidable necessity to characterize and assess every low-cost medium with respect to every
64 potential use.

65 This poses a significant challenge to researchers, as there is a substantial amount of work
66 involved in characterizing an adsorptive medium prior to its utilization in a real world
67 application. Batch studies, capable of providing a rough approximation of a medium's
68 adsorptive properties, are a common first step in media characterization, and these are an
69 attractive option by virtue of their being cheap and easy to perform, with experimental
70 methods being well established and results being easy to interpret (Crini and Badot, 2008).
71 The primary disadvantage is that batch experimental conditions are radically different to
72 through-flow conditions in real world filter-beds. These studies are, for this reason, unable to
73 provide sufficient information to allow for the design of full-scale adsorption filters (Søvik
74 and Kløve, 2005). Accordingly, when media are to be used in filter-beds, large-scale field
75 studies are widely considered to be the most reliable method of assessing their potential (Pratt
76 et al., 2012). Such tests provide excellent insight into the behavior of real-world adsorption
77 systems; however, the propriety of conducting such large-scale and costly investigations is
78 questionable when using untested and unproven materials. The limitations of both batch
79 studies and large-scale column studies have made rapid small-scale column tests (RSSCTs),
80 of the kind proposed by Crittenden et al. (1986, 1987), an ideal option for initial media

81 characterization, and it has been repeatedly demonstrated that such tests can provide excellent
82 predictions as to the performances of real-world filter units (Crittenden et al., 1991). RSSCTs
83 involve the use of scaling equations to select media particle sizes, hydraulic loading rates, and
84 empty bed contact times (EBCT, defined as the empty bed volume divided by the flow rate)
85 which will ensure exact similarity of operation between small- and large-scale adsorption
86 filters. Providing exact similitude is achieved, the breakthrough curve (BTC) observed when
87 operating a small-scale filter column should match that of a large-scale filter almost exactly.
88 The advantages of RSSCT type experiments are numerous; they are fast and inexpensive to
89 perform, they require minimal quantities of both adsorbent and adsorbate solution, and
90 perhaps most importantly, they investigate the interaction between adsorbent and adsorbate
91 under through-flow conditions which are representative of intended field conditions,
92 providing insight into both adsorption capacity and kinetics simultaneously. The primary
93 drawback of RSSCTs is that they only make reliable predictions for the very specific case for
94 which they were designed; a single RSSCT corresponds to only one large-scale filter
95 operated in an exactly similar manner (in terms of loading rate and empty bed contact time
96 etc). Also, while it is easy to obtain different particle sizes of activated carbon (the material
97 for which the RSSCT methodology was originally proposed), it may not be possible to scale
98 down many low-cost media due to their physical characteristics.

99 Mathematical models provide a means by which to make theoretical predictions for any
100 fixed-bed system, and there are a great many mathematical models which have been
101 developed in an attempt to predict the breakthrough behavior of adsorptive media. Xu et al.
102 (2013) summarized some of the most widely used of these in a recent review, listing,
103 amongst others, the Thomas model (Thomas, 1944), the Bohart-Adams (B-A) model (Bohart
104 and Adams, 1920), and the Bed Depth Service Time (BDST) model (Hutchins, 1973). It is
105 interesting to note that the B-A model is often erroneously referred to as the Thomas model;

106 this has caused considerable confusion (Chu, 2010), even though the former predates the
 107 latter by a considerable margin. The B-A model is also the basis of the popular BDST model
 108 proposed by Hutchins (1973), which is, essentially, just a simplified rearrangement of the B-
 109 A model. It therefore seems reasonable to assert that the B-A model is quite possibly the most
 110 popular fixed-bed sorption model in current use. The basic form of the B-A model is as
 111 follows:

$$112 \quad \ln\left(\frac{C_o}{C_b} - 1\right) = \ln\left[\exp\left(k_{BA}N_o\frac{Z}{U}\right) - 1\right] - k_{BA}C_o t_b \quad (1)$$

113 Where C_o is the influent concentration, C_b is the effluent breakthrough concentration at any
 114 time, t_b ; K_{BA} is a kinetic constant associated with the B-A model, N_o is the adsorptive
 115 capacity of the medium per unit volume of the bed, Z is the depth of medium in the filter bed,
 116 and U is the linear flow velocity.

117 In practice, $\exp(K_{BA}N_oZ/U)$ is often much larger than one (Al-Degs et al., 2009), and the
 118 equation can therefore be simplified by ignoring the unity term on the right hand side of
 119 Eqn.1 to yield:

$$120 \quad \ln\left(\frac{C_o}{C_b} - 1\right) = k_{BA}N_o\frac{Z}{U} - k_{BA}C_o t_b \quad (2)$$

121 As stated earlier, Hutchins' BDST model is based on a rearrangement of the simplified B-A
 122 equation (Eqn.2), and proposes a linear relationship between filter-bed depth and filter
 123 service time to a given breakthrough concentration. The time to any breakthrough
 124 concentration is found by rearranging Eqn. 2 into form $t=mx+c$, to yield Hutchins' BDST
 125 equation (Hutchins, 1973) as follows:

$$126 \quad t_b = \frac{N_o}{C_o U} Z - \frac{1}{K_{BA}C_o} \ln\left(\frac{C_o}{C_b} - 1\right) \quad (3)$$

127 Mathematical modelling offers more versatility in terms of predicting a wide range of
128 potential fixed-bed arrangements, though this is arguably at the cost of the certainty and
129 reliability that predictions based on experimental observations provide. It would therefore
130 seem logical that a combination of both experimental observation and mathematical
131 modelling would hold promise - providing the versatility of mathematical modelling as well
132 as the certainty associated with experimental results. The BDST modeling approach is a
133 widely implemented example of such a procedure. The BDST approach to filter design
134 involves using experimental data from a number of filter columns to determine the
135 coefficients N_0 and K_{BA} in Eqn. 3. The BDST model then allows for designers to use
136 interpolation and extrapolation to make predictions as to the behavior of adsorption systems
137 with different flow rates, bed depths, and influent concentrations to those used to obtain the
138 model coefficients.

139 The BDST model does not attempt to predict full BTCs, but instead predicts the time at
140 which a certain breakthrough concentration will occur for a given filter depth and flow rate.
141 Were the BDST equation rearranged in an attempt to predict the entire BTC, a sigmoidal
142 function would be obtained, i.e. Eqn. 2. Therefore, the BDST model may fit experimental
143 data at a single breakthrough point, but if extrapolations are made to different breakthrough
144 concentrations, predicted BTCs may vary significantly from observed BTCs. This is
145 particularly true in relation to low-cost adsorbents, which often produce BTCs that deviate
146 significantly from the ideal symmetrical sigmoidal shape predicted by formulae such as that
147 used in the BDST model.

148 Naturally, with the addition of enough modifying constants, a model can achieve an almost
149 perfect fit to any dataset, but this detracts from the purpose of creating a model; a model
150 should be simple enough to be of practical use, allowing for its easy application by those in
151 industry, but sophisticated enough that the predictions it offers will be of practical use.

152 Creating a model which adheres to these criteria will necessitate the adoption of various
153 simplifications and assumptions, and depending on the assumptions made, the resultant
154 model will almost certainly only be suitable for only certain adsorption systems (Xu et al.,
155 2013). This is not a limitation, per se, rather just an unavoidable reality, one that necessitates
156 the use of different models for different systems. Striving to create a ‘perfect’ model at the
157 expense of its ever being practically utilized is a wholly academic pursuit if its complexity is
158 such that very few can effectively implement it. This is reflected by the popularity of the
159 simple B-A model, which assumes a rectangular isotherm, while the Thomas model, which
160 assumes a more realistic Langmuir isotherm, and often offers a better fit to experimental data,
161 has seen much less use; Chu (2010) compared the Thomas model to the B-A model and
162 described the former as being “computationally intractable”.

163 In a recent paper, Callery et al. (2016) found that the long-term performance of large-scale
164 filters packed with low-cost adsorbents could be predicted mathematically using a simple
165 model, which was constructed using 24 hr of experimental data obtained from small-scale
166 column tests. The methods used didn’t require the use of scaling equations, as is generally the
167 case with RSSCTs. Similitude was achieved by using the same media particle sizes and
168 hydraulic loading rates in both the large and small-scale filters. In this way, the small
169 columns were not so much scaled-down versions of large-scale filters, rather they could be
170 considered cylindrical longitudinal-sections of hypothetical large-scale filter-beds. The BTCs
171 obtained from these small-scale filters could be modeled, and extrapolations could be made to
172 predict the performance of large-scale filters using the same media.

173 While dispensing with the necessity for scaling equations made this method simpler than the
174 RSSCT approach, the advantages of RSSCTs were retained. So too was the disadvantage that
175 there needed to be exact similarity between the small- and large-scale tests. For this reason,
176 there is a necessity to develop this method further before it is capable of predicting the

177 performance of filters with any bed depth operated at any loading rate, and this need is
178 addressed by this study.

179 **Theory**

180 In through-flow adsorption systems, the mass of adsorbate retained by a filter medium is a
181 function of the contact time between the adsorbent medium and the adsorbate solution. This
182 means that having an understanding of an adsorbent's kinetic performance is of paramount
183 importance when attempting to design any such system (Qiu et al., 2009). Changing the bed
184 depth of a filter-bed (or adjusting the hydraulic loading rate) will affect the EBCT (used as a
185 measure of the contact time between the adsorbent and the adsorbate solution) which will in
186 turn affect the system's performance. The BDST model supposes that the relationship
187 between bed depth (and therefore EBCT) and service time – the filter operating time to some
188 defined breakthrough concentration - is a linear one (Hutchins, 1973). This assumption, while
189 often reasonable, was quickly shown to not be valid for all systems (Poots et al., 1976a,
190 1976b). Curved plots of bed depth vs. service time are not uncommon, and intraparticle
191 diffusion can cause tailing of BTCs (Deokar and Mandavgane, 2015), and non-linear BDST
192 plots which deviate from those predicted by Hutchins' BDST model (Ko et al., 2000, 2002).
193 Internal diffusion of adsorbate molecules often becomes a significant factor as a medium's
194 surface becomes increasingly saturated, or as a result of lengthy filter EBCTs. Hutchins'
195 BDST model is based on the assumption that intraparticle diffusion and external mass
196 resistance are negligible (Ayoob and Gupta, 2007); this is rarely the case in real-world
197 adsorption systems, where adsorption is seldom controlled solely by surface chemical
198 reactions between the adsorbent and adsorbate (Crini and Badot, 2010). This limitation has
199 been noted before, and attempts have been made to modify the BDST model to make it more
200 universally applicable (Ko et al., 2000, 2002).

201 In deriving their fixed-bed model, Bohart and Adams (1920) made the assumption that the
202 rate of the adsorption reaction in a fixed bed filter is proportional to the fraction of the

203 medium's adsorption capacity which is still retained, and the concentration of adsorbate in
204 the solution being filtered. They described this relationship as follows:

$$205 \quad \frac{\partial N}{\partial t} = -kNC \quad (4)$$

$$206 \quad \frac{\partial C}{\partial Z} = \frac{-k}{U}NC \quad (5)$$

207 Where C is the adsorbate concentration of the solution being filtered, t the time, Z the filter
208 bed depth, U the flow velocity of the solution past the adsorbent, and k is a reaction rate
209 constant; N is the residual adsorption capacity which is assumed to be some fraction, N', of
210 the adsorptive capacity of the adsorbent, N_o (i.e. N'=N/N_o, or N=N_oN').

211 Eqns. 4 and 5 are based on the assumption that the filter bed has a definite sorption
212 maximum, N_o, which is independent of bed contact time and the duration for which the filter
213 has operated; at equilibrium Eqn. 4 reduces to a rectangular sorption isotherm (highly
214 favorable, irreversible adsorption) (Chu, 2010). In reality, it is known that filter-bed
215 adsorption capacity does change depending on the fluid residence time in the bed (Ko et al.,
216 2000, 2002) and the duration of filter operation. Increases in bed depth, and consequent
217 increases in EBCT and service time, allow adsorbate molecules to diffuse deeper into the
218 adsorbent particles resulting in a consequent increase in bed capacity. To account for this, Ko
219 et al. (2000, 2002) proposed that a time dependent bed capacity term, N_t, could replace the
220 standard bed capacity term of the BDST model, N_o, and presented two possible equations
221 with which to determine this value:

$$222 \quad N_t = N_o(1 - e^{-at}) \quad (6)$$

$$223 \quad N_t = N_o(1 - e^{-a^*\sqrt{t}}) \quad (7)$$

224 Where a and a* are first order and diffusional kinetic rate parameters respectively.

225 Regardless of the solid-liquid contact mechanism employed (i.e. batch or fixed bed), the
 226 equilibrium and kinetic characteristics of an adsorption system remain unchanged (Chu,
 227 2010). With this in mind, just as Eqn. 6 is based on Lagergren's (1898) pseudo first-order
 228 model, following the work of Liu (2008), another possible expression for N_t is proposed,
 229 based on Ho and McKay's (1999) pseudo second-order model:

$$230 \quad N_t = N_o \frac{t}{t+a^{**}} \quad (8)$$

231 Where a^{**} is a fitting parameter associated with second order kinetics; the full derivation of
 232 Eqn. 8 can be found accompanying Figure S1 of the supplementary information. It is worth
 233 noting that (given the interdependence of bed depth, EBCT, and service time), with different
 234 values for the constants a , a^* , and a^{**} , EBCT could be used in the place of service time, t , in
 235 Eqns. 6 - 8. The primary advantage of this being that EBCT is an easily calculable property
 236 of a filter, whereas service time must be experimentally determined. This point is also
 237 expounded in Figure S1 of the supplementary file accompanying this text.

238 When N_t (as defined by one of Eqns. 6, 7 or 8, to be selected on the basis of best fit to the
 239 system in question) is substituted for N_o in Eqn. 3, a modified form of the BDST equation
 240 (one which can describe a non-linear relationship between bed depth and service time) is
 241 obtained:

$$242 \quad t_b = \frac{N_t Z}{C_o U} - \frac{1}{k_{BA} C_o} \ln \left(\frac{C_o}{C_b} - 1 \right) \quad (9)$$

243 This equation can also be rearranged in the form of a modified BA equation to describe
 244 sigmoidal breakthrough curves:

$$245 \quad \ln \left(\frac{C_o}{C_b} - 1 \right) = \frac{k_{BA} N_t Z}{U} - k_{BA} C_o t_b \quad (10)$$

246 Ko et al. (2000, 2002) demonstrated the utility of this modified BDST model (Eqn. 9), using
247 Eqns. 6 and 7 to determine values for N_t (to the best of our knowledge, Eqn. 8 has not yet
248 been used for this purpose), however, once the model is rearranged in the form of Eqn. 10 an
249 inherent limitation becomes apparent: the model describes only sigmoidal curves, and is
250 therefore poorly suited to the description of linear to convex BTCs which are commonly
251 observed in fixed-bed studies using low-cost adsorbents.

252 To address this limitation, Callery et al. (2016) proposed the following model in a recent
253 study:

$$254 \quad C_e = C_o - \frac{q_e M}{VB} \quad (11)$$

255 Where C_e and C_o are the filter effluent and influent contaminant concentrations respectively,
256 M is the mass of filter medium, V is the volume of solution loaded on to the filter, B is a
257 model constant, and q_e is the mass of adsorbate adsorbed per unit mass of filter medium, as
258 modeled by:

$$259 \quad q_e = AV_B \left(\frac{1}{B} \right) \quad (12)$$

260 where A is a model constant and V_B is the number of bed volumes of solution filtered.

261 Callery et al. (2016) found that Eqns. 11 and 12 were well suited to the modeling of non-
262 sigmoidal BTCs, though a limitation of this model is that it does not provide any information
263 regarding the bed depth service time relationship. It is hypothesized that this may be easily
264 addressed; just as Ko et al. (2000, 2002) replaced N_o with N_t to modify the B-A/BDST
265 model, q_e in Eqn. 11/12 could be replaced with an analogous time dependent parameter, q_t .
266 Mirroring Eqns. 6-8, the following expressions for q_t are obtained:

$$267 \quad q_t = q_e(1 - e^{-at}) \quad (13)$$

268 $q_t = q_e(1 - e^{-a^*\sqrt{t}})$ (14)

269 $q_t = q_e \frac{t}{t+a^{**}}$ (15)

270 Again, a , a^* , and a^{**} are model constants associated with first order, diffusional, and second
271 order kinetics respectively. Their value in the above equations will depend on whether service
272 time or EBCT is used in the place of t ; EBCT will be used in this study.

273 The adsorbate solution's concentration will reduce as it travels through the filter bed and, if
274 the flow rate is constant, we can assume that at any depth within the filter, the pore
275 concentrations will depend on the contact time that has elapsed between the solution and the
276 filter medium, (as well as the duration for which the filter has been loaded). The solution
277 adsorbate concentration at any filter depth (i.e. after any EBCT), C_t , as opposed to the filter
278 effluent concentration, C_e , can be found by substituting q_t for q_e in Eqn 11/12:

279
$$C_t = C_o - \frac{q_t M}{VB}$$
 (16)

280 Given the linear relationship between filter depth and EBCT, Eqn. 16 can be used to calculate
281 the filter pore concentrations of the adsorbate solution at any depth within the filter-bed after
282 any filter loading, V , and can therefore describe the propagation of concentration fronts
283 within the filter-bed.

284 Eqn. 16 can also be rearranged to yield a function with similar utility to Hutchins' BDST
285 model, i.e. one that describes the relationship between bed depth and volume of solution
286 treated to any breakthrough concentration, C_t , of interest:

287
$$V = \frac{q_t M}{B(C_o - C_t)}$$
 (17)

288 The filter service time can be found from Eqn. 17 by dividing the volume treated, V (L), by
289 the loading rate ($L s^{-1}$).

290 In summary, sigmoidal BTCs and corresponding plots of bed depth vs. service time may be
291 described by Eqns. 10 and 9 respectively, while linear to convex BTCS and corresponding
292 plots of bed depth vs. service time may be described by Eqns. 17 and 16 respectively.

293 **Materials and Methods**

294 **Preparation of filter columns**

295 The low-cost adsorbents utilized in this study were aluminum water treatment residual (dried
296 at 105°C for 24 hr and ground to pass a 0.5 mm sieve) and two grades of crushed concrete
297 (“fine”, ground to pass 0.5 mm sieve, and “coarse”, ground to pass a 1.18 mm sieve but
298 retained by a 0.5 mm sieve). Small bore filter columns of lengths 0.1, 0.15, 0.2, 0.3, and 0.4
299 m were constructed using HDPE tubing with an internal diameter of 0.0094 m. These
300 columns were packed with each of the aforementioned media, with care being taken to ensure
301 that an equal bulk density was achieved in each filter. Endcaps, consisting of PE syringe
302 barrels packed with a small quantity of glass wool, were fastened by means of a friction fit to
303 the ends of the filter columns, and silicone tubing was connected to the tip of these syringe
304 barrels to provide inlet and outlet lines to the filter columns. Large bore filter columns of
305 length 0.65 m were then constructed in triplicate using uPVC piping with an internal diameter
306 of 0.104 m. These columns were packed to a bed depth of 0.4 m using the same media and
307 same packing density as was used in the small-bore filters. Again, care was taken to ensure
308 that an equal bulk density was achieved in each filter for each medium. Sampling ports were
309 installed through the walls of the large-bore filter columns at bed depths of 0.05, 0.1, 0.18,
310 and 0.25 m from the filter surface. Water samples could also be collected from the outlet at
311 the base of each column.

312 **Operation of filter units**

313 A synthetic wastewater was produced by dissolving K_2HPO_4 in tap water to obtain a PO_4-P
314 concentration of 1 mg L^{-1} [similar to forest drainage water (Finnegan et al., 2012)]. A
315 peristaltic pump was used to supply this wastewater to the small-bore filter units at consistent
316 flow rates of between 134 and 259 mL hr^{-1} [hydraulic loading rates similar to those found in

317 high rate trickling filters (Spellman, 2013) or activated carbon adsorbers (Chowdhury, 2013)]
318 to achieve a variety of filter bed contact times. The small-bore filters were operated
319 intermittently, in 12 hour on/off cycles, and were fed from the bottom of the vertically
320 oriented filters to preclude any incidence of wastewater bypassing the filter media. The
321 effluent from the small-bore columns was collected in 2 hr aliquots using an auto-sampler.
322 The large-bore filter columns were manually loaded 2-3 days per week with 28 L of the same
323 synthetic wastewater as used in the small-bore filters. Water samples were collected from the
324 sampling ports at various intervals, and the effluent from each loading event was collected in
325 large HDPE containers.

326 **Data collection and analysis**

327 Collected effluent samples were passed through 0.45 μm filters and analyzed with a Konelab
328 nutrient analyzer in accordance with the standard methods (Eaton et al., 1998). With the
329 influent and effluent $\text{PO}_4\text{-P}$ concentrations determined, medium saturation, q_e , was
330 calculated. Graphs of q_e vs V and C_e vs V were plotted, and Eqn.15 and Eqn.16 were fit to
331 these experimental data by non-linear regression, using Microsoft Excel's solver add-in to
332 minimize the sum of the squares of the errors (ERRSQ):

$$333 \quad \sum_{i=1}^p (q_{e,calc} - q_{e,meas})_i^2 \quad (18)$$

334 Where $q_{e,calc}$ is the model predicted equilibrium solid phase $\text{PO}_4\text{-P}$ concentration and $q_{e,meas}$ is
335 the measured equilibrium solid phase $\text{PO}_4\text{-P}$ concentration.

336 **Predicting large-scale filter performance**

337 With the coefficients A , B , and a^{**} determined from the small-scale column tests, Eqn. 16
338 was used to predict effluent concentrations and pore water concentrations at multiple depths
339 within the large-scale filter columns. V_x , the volume of the large-scale filter to a depth of 'x'

340 was calculated by multiplying 'x' by the area of the filter column (i.e. $\pi D^2/4$, where D is
341 0.104m, the internal diameter of the large-scale filter column). After some filter loading, V,
342 the pore concentration at a filter-bed depth of 'x' (if predicting effluent concentration, $x=Z$,
343 the full filter-bed depth), was predicted by inputting the following values into Eqn. 16: $V_B =$
344 V/V_x , $M = \rho V_x$ (where ρ is the bulk density of the media in the filter column; this should be
345 the same as used in the small-scale tests), and $t = V_x/Q$ (where Q is the loading rate applied to
346 the large-scale filter).

347 **Validation of model using independent data**

348 To validate and further support the modelling strategy applied in this study, a literature
349 review was carried out to identify column studies which utilized low-cost adsorbents and
350 observed BTCs which tended towards a convex to linear shape, rather than the sigmoidal
351 curve predicted by other models. The BTCs published in these studies were downloaded as
352 raster images and converted to vector graphics, the ordinates of which could be exported as a
353 text file. The text files were imported into Microsoft Excel as x and y coordinates, which
354 could then be processed in the same fashion as the experimental data. This method was
355 validated using known data points, and it was found that the mean absolute percentage error
356 between actual values and data points obtained in this manner was 0.18%.

357 Figure 1 shows a step-by-step schematic of the data collection and modelling procedure
358 employed in this study.

359 **4. Results and Discussion**

360 **Predicting medium saturation in RSSCTs**

361 Figure 2 shows plots of filter loading versus phosphorus retained by filter columns of various
362 lengths. As can be seen, the relationship between filter loading and medium saturation could
363 be accurately described by Eqn. 15. The ERRSQ function was used as a metric for goodness
364 of model fit, with average ERRSQ values of 0.074, 0.057, and 0.008 obtained for small-scale
365 filter columns containing Al-WTR, fine concrete, and coarse concrete, respectively. As
366 described previously, q_t can be calculated in a number of ways; Figure S2 in the
367 supplementary file compares graphs of the three functions from which a value for q_t may be
368 obtained. Comparing the shapes of these functions, it can be seen that Eqn. 14, originally
369 proposed by Ko et. al (2000, 2002) to account for diffusional adsorption, appears to very
370 closely match the curve produced by Eqn. 15, based on second-order kinetics. This would
371 seem to indicate that both functions might have similar utility, however the differences
372 between the two can be considerable when the two are compared on a local scale, as can be
373 seen from the inset in Figure S2. In constructing Figure 2, attempts were made to fit the
374 experimental data from the small-scale column tests to each of Eqns.13, 14 and 15. As can be
375 seen from Table 1, which compares ERRSQ values obtained using each of these equations,
376 Eqn. 15 was found to be optimal for each of the media studied. As it provided the best fit to
377 these initial data (and because Ko et al. (2000, 2002) have already explored the use of Eqns.
378 13 and 14), Eqn. 15 was used for the remainder of this study when fitting Eqns. 16 and 17 to
379 experimental data.

380 **Predicting pore concentrations at multiple depths in large-scale filter columns**

381 Once it was established that Eqn.15 was capable of describing and predicting the progression
382 of medium saturation in small-scale filter columns of various lengths, it was hypothesized

383 that Eqn.16 would also be able to predict pore $\text{PO}_4\text{-P}$ concentrations at any bed depth within
384 the filter bed of a large-scale column. To test this hypothesis, Eqn. 16 (with q_t determined
385 using Eqn. 15) was fit, using the ERRSQ method, to the data obtained from depth samples
386 taken from various depths within the large-scale filter columns. Figure 3(a) shows the fit of
387 Eqn. 16 to these experimental data, and the associated ERRSQ values are shown in Table 2.
388 Average ERRSQ values of 0.026, 0.011, and 0.005 were obtained for large-scale filter
389 columns containing Al-WTR, fine concrete, and coarse concrete, respectively. It can be seen
390 that the slight day-to-day variances in influent concentration had a marked influence on the
391 shape of the observed BTCs. While Eqn.16 was initially proposed to be accurate with the
392 assumption of constant influent concentration, it appeared to display good resilience to these
393 fluctuations, and was nonetheless able to make accurate pore and effluent concentration
394 predictions. With it established that the model could describe the performance of both small-
395 and large-scale filter columns, it was further hypothesized that the coefficients determined
396 from the small-scale columns could also be used to predict the performance of the large-scale
397 filter columns. With these coefficients, the performance of small-scale filters of any depth
398 operated at any HLR could be predicted, and equivalent loadings for large-scale columns
399 subjected to the same HLR were calculated by scaling filter throughput based on the ratio of
400 the small- and large-scale filter areas. Figure 3(b) shows data from the large-scale column
401 tests fit to models created using data from the small-scale column tests, and the associated
402 ERRSQ values are shown in Table 2. While not fitting quite as closely as when modeled
403 directly on the large-scale column data, the level of precision achieved was still very good,
404 with average ERRSQ values of 0.062, 0.054, and 0.008 obtained for filter columns containing
405 Al-WTR, fine concrete, and coarse concrete, respectively. For practical purposes of
406 preliminary filter design, this level of accuracy was considered more than sufficient, and it
407 allowed for prediction of the adsorptive performance of the large-scale filter columns for the

408 entire duration of their operation. It could reasonably be expected that loading the large-scale
409 filters with a wastewater whose chemical composition was significantly different from that of
410 the wastewater applied to the small-scale filters (in terms of pH, concentration of target
411 contaminant, competing compounds etc.) would invalidate any model predictions of large-
412 scale performance based on the small-scale experiments; a more complex modeling approach
413 would be required to take account of such variations.

414 **Validation of model using independent data**

415 To further verify the validity and utility of Eqn. 16, it was fit to BTCs published in a number
416 of independent studies. The results of this are shown in Figure 4, and it can be seen that the
417 model fit these data very well. Poots (1976b) was the first author who attempted to apply
418 Hutchins' (1973) BDST model to experimental results (according to the Web of ScienceTM
419 citation index), and found that it was a poorly suited to describing the relationship between
420 bed depth and service time in peat filters designed to remove Telon blue from aqueous
421 solution. However, as can be seen in Figure 4(a), Eqn. 16 was able to describe the
422 breakthrough behavior of Telon blue at all filter depths, accurately describing the non-linear
423 relationship between bed depth and service time described by the BTCs. A recent study on
424 phosphate adsorption (Nguyen et al., 2015) recorded BTCs from filters packed with a low
425 cost adsorbent (zirconium loaded okara) using phosphate concentrations an order of
426 magnitude higher than those used in the present study; as can be seen from Figure 4(b), Eqn.
427 16 was well suited to the description of these curves. Finally, Han et al. (2009) investigated
428 the ability of iron oxide-coated zeolite as an adsorbent for the removal of copper (II) from
429 aqueous solution in filter beds of various depths, and, as shown in Figure 4(c), the BTCs
430 obtained these can be suitably modeled by Eqn. 16.

431 **Description of sigmoidal curves**

432 Although Eqn.15 can describe many of the linear to convex BTCs commonly observed from
433 fixed-bed studies using low-cost adsorbents, it is not suitable for the description of sigmoidal
434 curves. This is perhaps the most commonly observed BTC shape observed in fixed-bed
435 sorption studies (Gupta et al., 2000), and so, an attempt was made to model curves of this
436 shape by modifying the B-A model (Eqn. 2) to obtain Eqn. 10, as described previously.
437 Using Eqn. 8 (letting t in Eqn. 8 be EBCT) to determine a value for N_t , Eqn. 10 was fit to a
438 number of independent data sets, as shown in Figure 5. In the B-A model, N_o serves a similar
439 function to q_e in Eqn. 11, as both represent the sorption capacity of the media. The B-A
440 model assumes a rectangular sorption isotherm (highly favorable, irreversible adsorption) and
441 a definite sorption maximum, which is independent of the contact time and the duration for
442 which the filter has operated. However, in reality, it is known that filter-bed adsorption
443 capacity does change depending on contact time (Ko et al., 2002) and duration of operation.
444 Eqn. 11 assumes that there is an exponential distribution of adsorption sites and energies,
445 meaning that adsorption energies become exponentially weaker with increasing duration of
446 filter operation and associated medium saturation; the bed's capacity increases with operating
447 time and, though there is no defined maximum capacity, there are adsorption maxima for any
448 given filter runtime. Making bed capacity dependent on empty bed contact time, i.e.
449 substituting q_t for q_e , proved to be very successful, and similar success was found modifying
450 Eqn. 2 by replacing N_o with N_t . This can be seen in Figure 5, in which Eqn.10 (with N_t
451 determined from Eqn. 8) has been fit to six independent data sets. Ko et al. (2000, 2002) also
452 implemented a similar approach, using Eqn. 6 and Eqn. 7 to modify the BDST model, which
453 is itself derived from the B-A model.

454 **Prediction of BDST relationship**

455 The relationship between bed depth and service time is not necessarily a linear one; greater
456 bed depths result in longer EBCTs, which in turn allow for increased adsorption due to

457 increased intraparticle diffusion of adsorbate molecules. Figure S3 of the supplementary file
458 shows some hypothetical BTCs, comparing a linear relationship between bed depth and
459 service time, as proposed by Hutchins' arrangement of the the B-A equation (Figure S3a),
460 and a non-linear relationship between bed depth and service time as predicted by Eqn. 10, the
461 B-A equation modified with Eqn. 8 (Figure S3b). The non-linear relationship between bed
462 depth and service time as predicted by Eqns. 16 and 17 is also shown in Figure S3b,
463 illustrating that the BDST plot doesn't necessarily provide any information regarding the
464 shape of the BTC; though the BTCs predicted by Eqn. 10 and Eqn. 16 are very different, both
465 yield the same curved BDST plot.

466 Ko et al. (Ko et al., 2002) modified the BDST model using Eqn. 6 and Eqn. 7, and this made
467 it possible to describe non-linear BDST plots. However, as can be seen in Figure 6, the BTCs
468 observed in their study were not sigmoidal, and so, the B-A model on which the modified
469 BDST model is based would not be appropriate for the description of entire BTCs. Eqn. 16
470 was fit to the data from this study, and, as can be seen in Figure 6, it was capable of
471 describing not only the non-linear BDST relationship, but also the entire BTC for each filter-
472 bed depth investigated. Eqn. 17 can therefore, in this case, be used to predict the BDST
473 relationship at any breakthrough concentration of interest, as well as at any flow rate of
474 interest, as demonstrated in Figure 6b.

475 **Conclusions**

476 This study described a testing and modelling methodology which uses results from
477 short-term small-scale column tests to predict the long-term performance of large-
478 scale fixed-bed filters.

- 479 • The proposed methodology was used to describe the adsorptive performance
480 of small-scale and large-scale filter columns, successfully modelling medium
481 saturation, as well as filter-pore and effluent concentration data.
- 482 • Predictions of large-scale filter performance based on small-scale filter
483 performance were highly accurate.
- 484 • Two three-parameter models were investigated, and these allowed for the
485 description and prediction of sigmoidal or convex breakthrough curves for
486 multiple filters containing the same media, as well as concentration profiles
487 across multiple depths within single filters.
- 488 • The proposed models also allow for the description of non-linear relationships
489 between filter-bed depth and service time, as is commonly observed in fixed-
490 bed systems which take a long time to reach equilibrium.
- 491 • The proposed modelling approach was applied to multiple independent data
492 sets and was found to suitably describe the adsorption of various solutes
493 including dyes, phosphate, metals (copper, cadmium, and zinc), fluoride, and
494 arsenic.

495 **Acknowledgement**

496 The first author would like to acknowledge the Irish Research Council (GOIPG/2013/75) for
497 funding.

- 499 Al-Degs, Y.S., Khraisheh, M.A.M., Allen, S.J., Ahmad, M.N., 2009. Adsorption characteristics of
500 reactive dyes in columns of activated carbon. *J. Hazard. Mater.* 165, 944–949.
501 doi:10.1016/j.jhazmat.2008.10.081
- 502 Ayoob, S., Gupta, A.K., 2007. Sorptive response profile of an adsorbent in the defluoridation of
503 drinking water. *Chem. Eng. J.* 133, 273–281. doi:10.1016/j.cej.2007.02.013
- 504 Babel, S., Kurniawan, T.A., 2003. Low-cost adsorbents for heavy metals uptake from contaminated
505 water: a review. *J. Hazard. Mater.* 97, 219–243. doi:10.1016/S0304-3894(02)00263-7
- 506 Bailey, S.E., Olin, T.J., Bricka, R.M., Adrian, D.D., 1999. A review of potentially low-cost sorbents for
507 heavy metals. *Water Res.* 33, 2469–2479. doi:10.1016/S0043-1354(98)00475-8
- 508 Bockris, J.O.M., Conway, B.E., White, R.E., 1995. *Modern aspects of electrochemistry* Vol. 29.
509 Springer.
- 510 Bohart, G.S., Adams, E.Q., 1920. Some Aspects of the Behavior of Charcoal with Respect to Chlorine.
511 1. *J. Am. Chem. Soc.* 42, 523–544. doi:10.1021/ja01448a018
- 512 Brown, P., Atly Jefcoat, I., Parrish, D., Gill, S., Graham, E., 2000. Evaluation of the adsorptive capacity
513 of peanut hull pellets for heavy metals in solution. *Adv. Environ. Res.* 4, 19–29.
514 doi:10.1016/S1093-0191(00)00004-6
- 515 Callery, O., Healy, M.G., Rognard, F., Barthelemy, L., Brennan, R.B., 2016. Evaluating the long-term
516 performance of low-cost adsorbents using small-scale adsorption column experiments.
517 *Water Res.* 101, 429–440. doi:10.1016/j.watres.2016.05.093
- 518 Chen, N., Zhang, Z., Feng, C., Li, M., Chen, R., Sugiura, N., 2011. Investigations on the batch and fixed-
519 bed column performance of fluoride adsorption by Kanuma mud. *Desalination* 268, 76–82.
520 doi:10.1016/j.desal.2010.09.053
- 521 Chowdhury, Z.K., 2013. *Activated Carbon: Solutions for Improving Water Quality*. American Water
522 Works Association.
- 523 Chu, K.H., 2010. Fixed bed sorption: Setting the record straight on the Bohart–Adams and Thomas
524 models. *J. Hazard. Mater.* 177, 1006–1012. doi:10.1016/j.jhazmat.2010.01.019
- 525 Crini, G., 2006. Non-conventional low-cost adsorbents for dye removal: a review. *Bioresour. Technol.*
526 97, 1061–1085.
- 527 Crini, G., Badot, P.-M., 2010. *Sorption Processes and Pollution: Conventional and Non-conventional*
528 *Sorbents for Pollutant Removal from Wastewaters*. Presses Univ. Franche-Comté.
- 529 Crini, G., Badot, P.-M., 2008. Application of chitosan, a natural aminopolysaccharide, for dye removal
530 from aqueous solutions by adsorption processes using batch studies: A review of recent
531 literature. *Prog. Polym. Sci.* 33, 399–447. doi:10.1016/j.progpolymsci.2007.11.001
- 532 Crittenden, J.C., Berrigan, J.K., Hand, D.W., 1986. Design of rapid small-scale adsorption tests for a
533 constant diffusivity. *J. Water Pollut. Control Fed.* 312–319.
- 534 Crittenden, J.C., Berrigan, J.K., Hand, D.W., Lykins, B., 1987. Design of rapid fixed-bed adsorption
535 tests for nonconstant diffusivities. *J. Environ. Eng.* 113, 243–259.
- 536 Crittenden, J.C., Reddy, P.S., Arora, H., Trynoski, J., Hand, D.W., Perram, D.L., Summers, R.S., 1991.
537 Predicting GAC Performance With Rapid Small-Scale Column Tests. *J. Am. Water Works*
538 *Assoc.* 83, 77–87.
- 539 Dąbrowski, A., 2001. Adsorption — from theory to practice. *Adv. Colloid Interface Sci.* 93, 135–224.
540 doi:10.1016/S0001-8686(00)00082-8
- 541 Deokar, S.K., Mandavgane, S.A., 2015. Estimation of packed-bed parameters and prediction of
542 breakthrough curves for adsorptive removal of 2,4-dichlorophenoxyacetic acid using rice
543 husk ash. *J. Environ. Chem. Eng.* 3, 1827–1836. doi:10.1016/j.jece.2015.06.025
- 544 Eaton, A.D., Clesceri, L.S., Greenberg, A.E., Franson, M.A.H., American Public Health Association.,
545 American Water Works Association., Water Environment Federation., 1998. *Standard*
546 *methods for the examination of water and wastewater*. American Public Health Association,
547 Washington, DC.
- 548 Faust, S.D., Aly, O.M., 1998. *Chemistry of Water Treatment*, Second Edition. CRC Press.
- 549 Finnegan, J., Regan, J.T., de Eyto, E., Ryder, E., Tiernan, D., Healy, M.G., 2012. Nutrient dynamics in a
550 peatland forest riparian buffer zone and implications for the establishment of planted
551 saplings. *Ecol. Eng.* 47, 155–164. doi:10.1016/j.ecoleng.2012.06.023

552 Futalan, C.M., Kan, C.-C., Dalida, M.L., Pascua, C., Wan, M.-W., 2011. Fixed-bed column studies on
553 the removal of copper using chitosan immobilized on bentonite. *Carbohydr. Polym.* 83, 697–
554 704. doi:10.1016/j.carbpol.2010.08.043

555 Goel, J., Kadirvelu, K., Rajagopal, C., Kumar Garg, V., 2005. Removal of lead(II) by adsorption using
556 treated granular activated carbon: Batch and column studies. *J. Hazard. Mater.* 125, 211–
557 220. doi:10.1016/j.jhazmat.2005.05.032

558 Gupta, V.K., Srivastava, S.K., Tyagi, R., 2000. Design parameters for the treatment of phenolic wastes
559 by carbon columns (obtained from fertilizer waste material). *Water Res.* 34, 1543–1550.
560 doi:10.1016/S0043-1354(99)00322-X

561 Han, R., Zou, L., Zhao, X., Xu, Y., Xu, F., Li, Y., Wang, Y., 2009. Characterization and properties of iron
562 oxide-coated zeolite as adsorbent for removal of copper(II) from solution in fixed bed
563 column. *Chem. Eng. J.* 149, 123–131. doi:10.1016/j.cej.2008.10.015

564 Ho, Y.S., McKay, G., 1999. Pseudo-second order model for sorption processes. *Process Biochem.* 34,
565 451–465. doi:10.1016/S0032-9592(98)00112-5

566 Hutchins, R., 1973. New method simplifies design of activated carbon systems, Water Bed Depth
567 Service Time analysis. *J Chem Eng Lond* 81, 133–138.

568 Ko, D.C.K., Lee, V.K.C., Porter, J.F., McKay, G., 2002. Improved design and optimization models for
569 the fixed bed adsorption of acid dye and zinc ions from effluents. *J. Chem. Technol.*
570 *Biotechnol.* 77, 1289–1295. doi:10.1002/jctb.707

571 Ko, D.C.K., Porter, J.F., McKay, G., 2000. Optimised correlations for the fixed-bed adsorption of metal
572 ions on bone char. *Chem. Eng. Sci.* 55, 5819–5829. doi:10.1016/S0009-2509(00)00416-4

573 Kumar, U., Bandyopadhyay, M., 2006. Fixed bed column study for Cd(II) removal from wastewater
574 using treated rice husk. *J. Hazard. Mater.* 129, 253–259. doi:10.1016/j.jhazmat.2005.08.038

575 Kundu, S., Gupta, A.K., 2005. Analysis and modeling of fixed bed column operations on As(V)
576 removal by adsorption onto iron oxide-coated cement (IOCC). *J. Colloid Interface Sci.* 290,
577 52–60. doi:10.1016/j.jcis.2005.04.006

578 Lagergren, S., 1898. About the theory of so-called adsorption of soluble substances.

579 Liu, Y., 2008. New insights into pseudo-second-order kinetic equation for adsorption. *Colloids Surf.*
580 *Physicochem. Eng. Asp.* 320, 275–278. doi:10.1016/j.colsurfa.2008.01.032

581 Maliyekkal, S.M., Sharma, A.K., Philip, L., 2006. Manganese-oxide-coated alumina: A promising
582 sorbent for defluoridation of water. *Water Res.* 40, 3497–3506.
583 doi:10.1016/j.watres.2006.08.007

584 Nguyen, T.A.H., Ngo, H.H., Guo, W.S., Pham, T.Q., Li, F.M., Nguyen, T.V., Bui, X.T., 2015. Adsorption
585 of phosphate from aqueous solutions and sewage using zirconium loaded okara (ZLO): Fixed-
586 bed column study. *Sci. Total Environ.* 523, 40–49. doi:10.1016/j.scitotenv.2015.03.126

587 Poots, V.J.P., McKay, G., Healy, J.J., 1976a. The removal of acid dye from effluent using natural
588 adsorbents—II Wood. *Water Res.* 10, 1067–1070. doi:10.1016/0043-1354(76)90037-3

589 Poots, V.J.P., McKay, G., Healy, J.J., 1976b. The removal of acid dye from effluent using natural
590 adsorbents—I peat. *Water Res.* 10, 1061–1066. doi:10.1016/0043-1354(76)90036-1

591 Pratt, C., Parsons, S.A., Soares, A., Martin, B.D., 2012. Biologically and chemically mediated
592 adsorption and precipitation of phosphorus from wastewater. *Curr. Opin. Biotechnol.*,
593 *Phosphorus biotechnology • Pharmaceutical biotechnology* 23, 890–896.
594 doi:10.1016/j.copbio.2012.07.003

595 Qiu, H., Lv, L., Pan, B., Zhang, Qing-jian, Zhang, W., Zhang, Quan-xing, 2009. Critical review in
596 adsorption kinetic models. *J. Zhejiang Univ. Sci. A* 10, 716–724. doi:10.1631/jzus.A0820524

597 Reddad, Z., Gerente, C., Andres, Y., Le Cloirec, P., 2002. Adsorption of Several Metal Ions onto a Low-
598 Cost Biosorbent: Kinetic and Equilibrium Studies. *Environ. Sci. Technol.* 36, 2067–2073.
599 doi:10.1021/es0102989

600 Søvik, A.K., Kløve, B., 2005. Phosphorus retention processes in shell sand filter systems treating
601 municipal wastewater. *Ecol. Eng.* 25, 168–182. doi:10.1016/j.ecoleng.2005.04.007

602 Spellman, F.R., 2013. *Handbook of Water and Wastewater Treatment Plant Operations*, Third
603 Edition. CRC Press.

604 Thomas, H.C., 1944. Heterogeneous Ion Exchange in a Flowing System. *J. Am. Chem. Soc.* 66, 1664–
605 1666. doi:10.1021/ja01238a017

- 606 Wong, K.K., Lee, C.K., Low, K.S., Haron, M.J., 2003. Removal of Cu and Pb from electroplating
607 wastewater using tartaric acid modified rice husk. *Process Biochem.* 39, 437–445.
608 doi:10.1016/S0032-9592(03)00094-3
- 609 Xu, Z., Cai, J., Pan, B., 2013. Mathematically modeling fixed-bed adsorption in aqueous systems. *J.*
610 *Zhejiang Univ. Sci. A* 14, 155–176.

Figures

Figure 1. Step-by-step schematic of the data collection and modelling procedure employed in this study.

Figure 2. Phosphorus retained by filter media (y-axis) vs. filter loading (x-axis) for small scale filter columns of various lengths and predictions made by Equation 15.

Figure 3. PO₄-P concentration (y-axis) vs. filter loading (x-axis) for large scale filter columns, showing (a) Equation 16 fit directly to large scale column data , and (b) predictions made by Equation 16 with model coefficients determined from small-scale column tests.

Figure 4. Equation 16 fit to independent data sets of normalised pore/effluent contaminant concentration (y-axis) vs. filter loading/operating time (x-axis).

Figure 5. Equation 10 fit to independent data sets of normalised pore/effluent contaminant concentration (y-axis) vs. filter loading/operating time (x-axis).

Figure 6. (a) Equation 16 fit to an independent data set of normalised effluent contaminant concentration (y-axis) vs. filter operating time (x-axis) for various filter-bed depths, and (b) plots of filter service-time (y-axis) vs. filter-bed depth (x-axis) compared to predictions made by Equation 17 using the same model coefficients

Tables

Table 1. ERRSQ values obtained using Equations 13, 14, and 15 to model phosphorus retained by filter media vs. filter loading for small-scale filter columns of various lengths.

Table 2. Comparison of model coefficients and ERRSQ values obtained when (a) fitting Equation 16 directly to concentration data from the large-scale column experiments and (b) when fitting Eqn. 16 to concentration data from the large-scale column experiments using model coefficients determined from small-scale column tests.

Figure 1

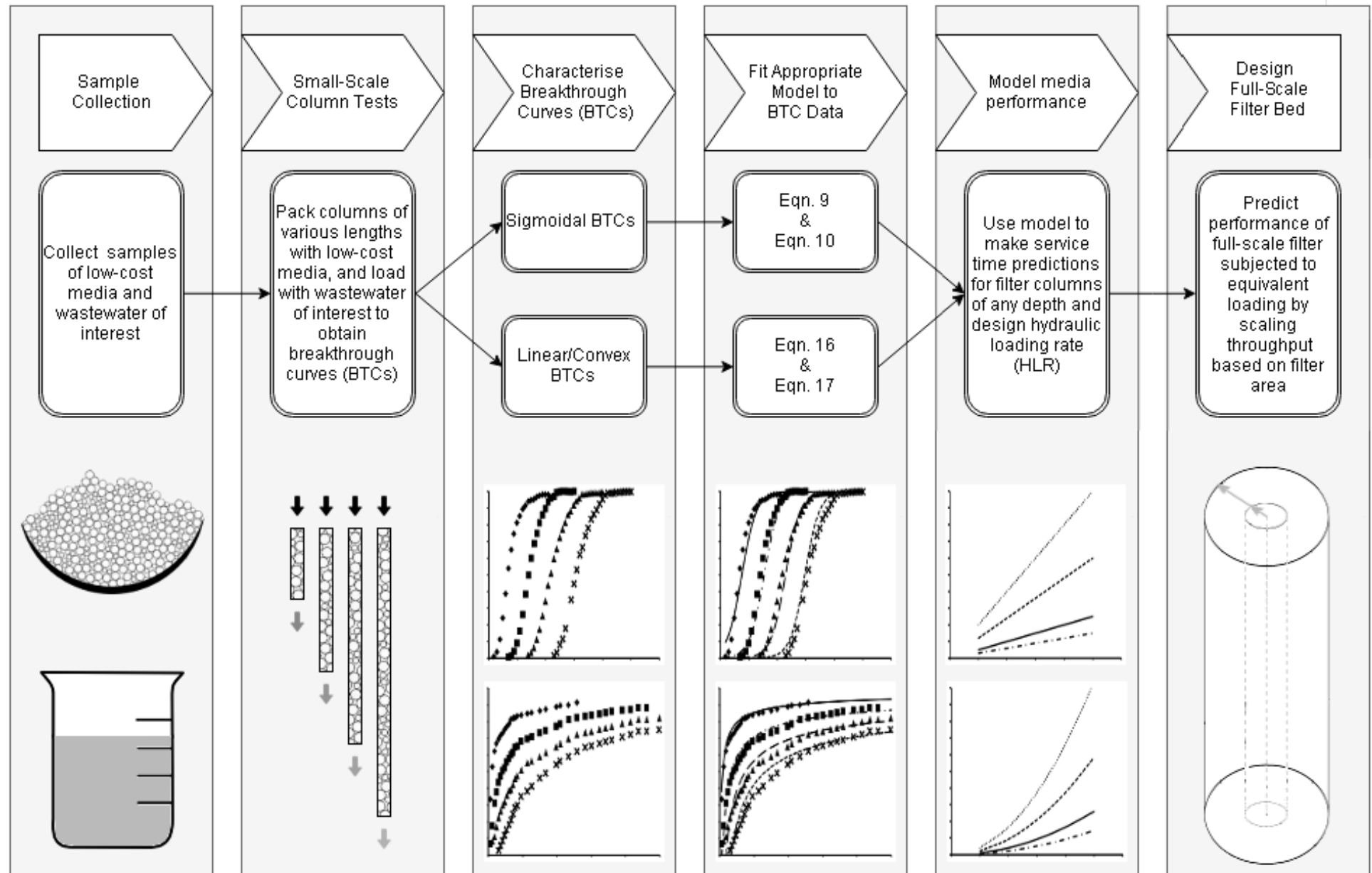


Figure 2

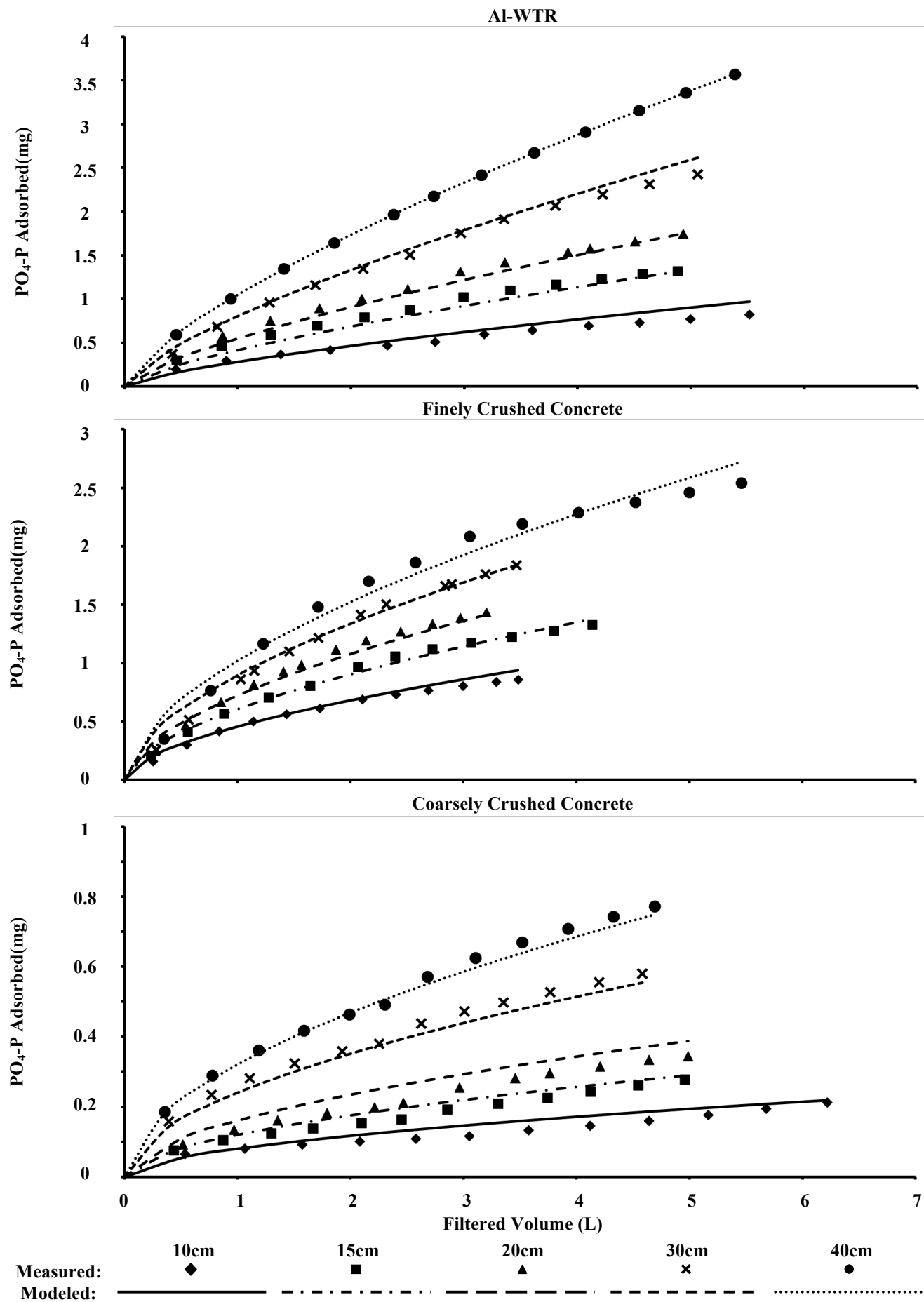


Figure 3

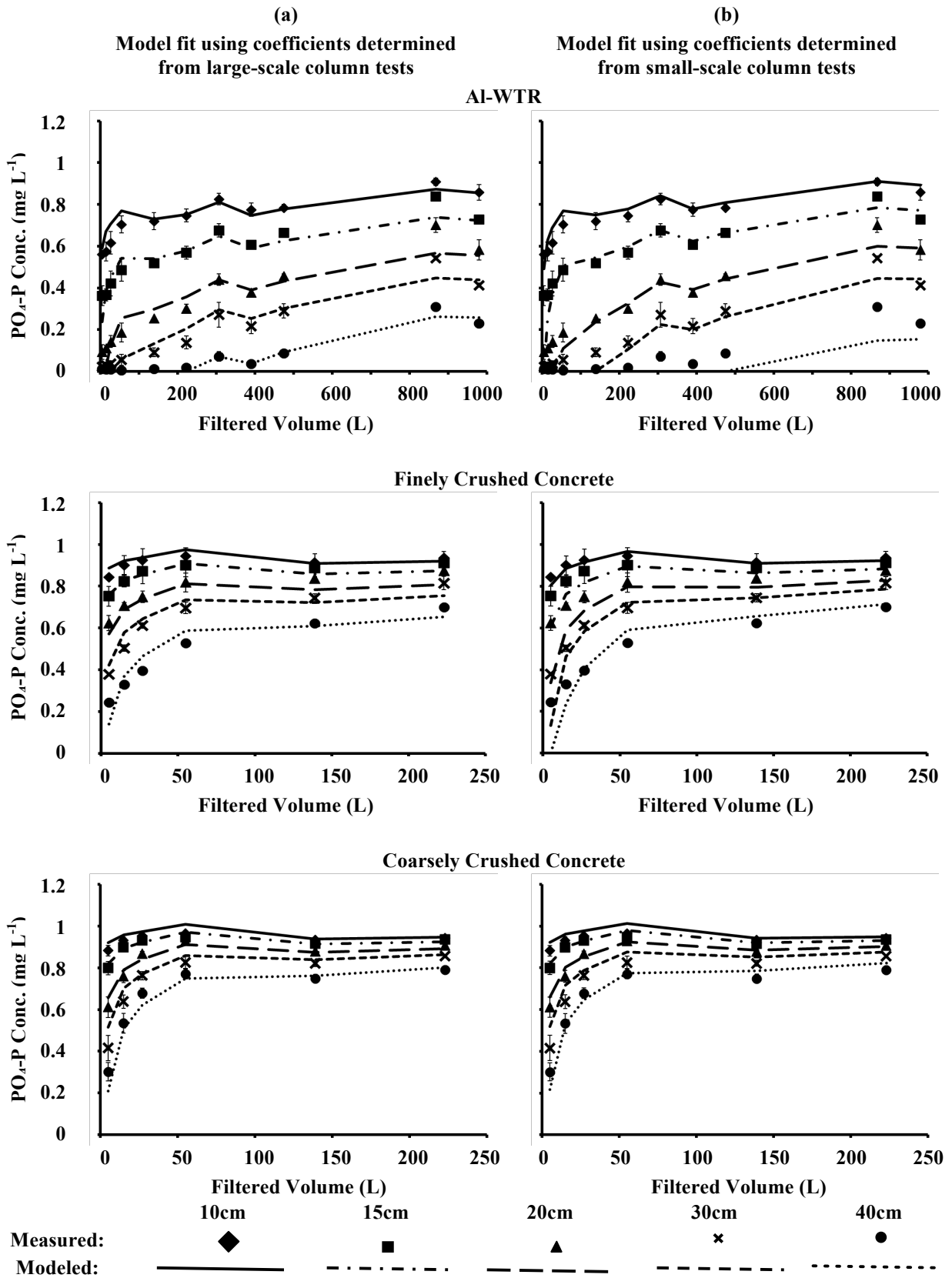


Figure 4

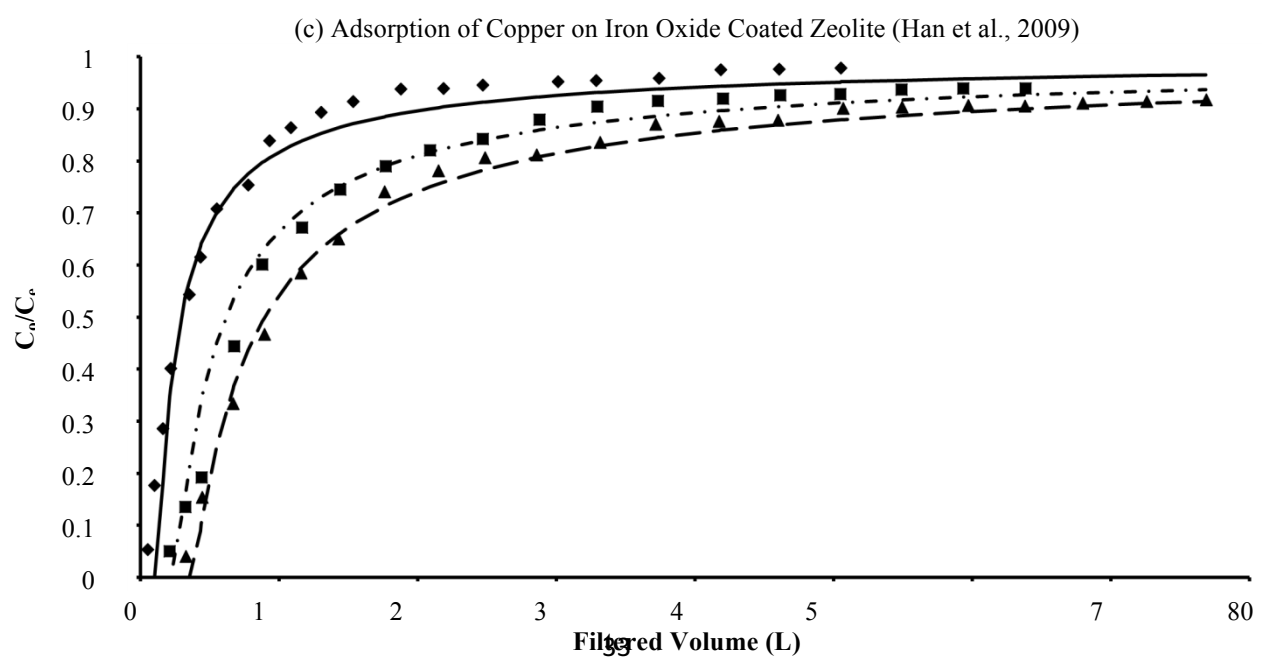
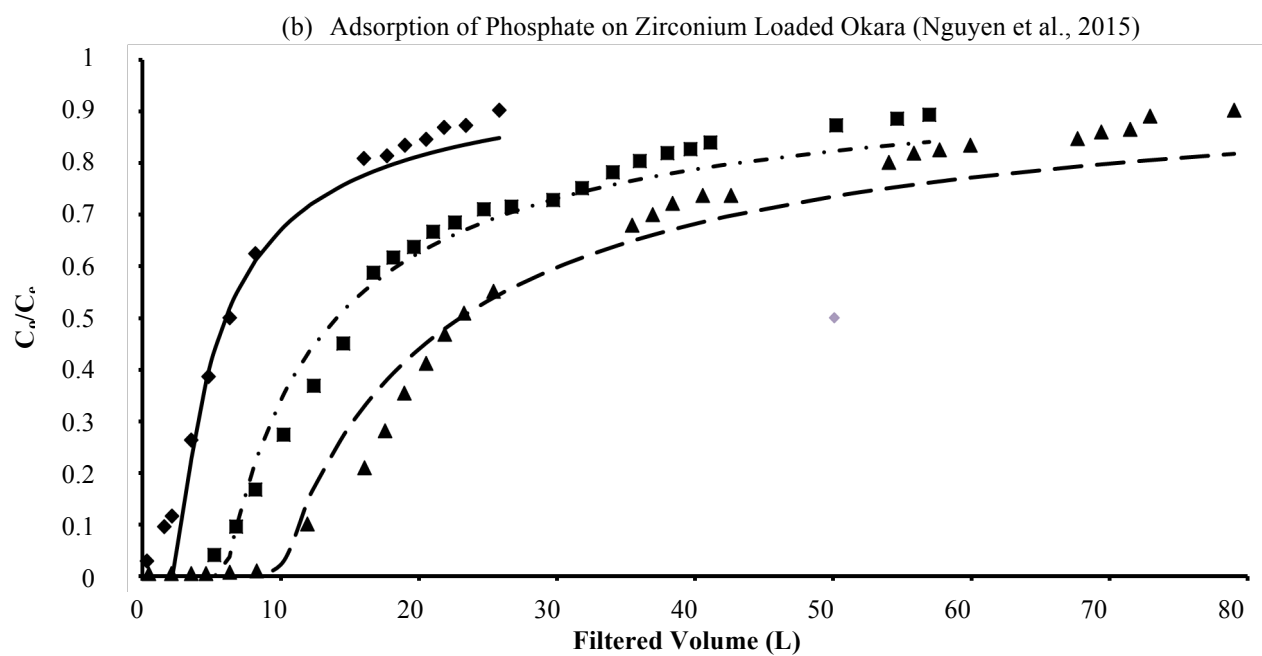
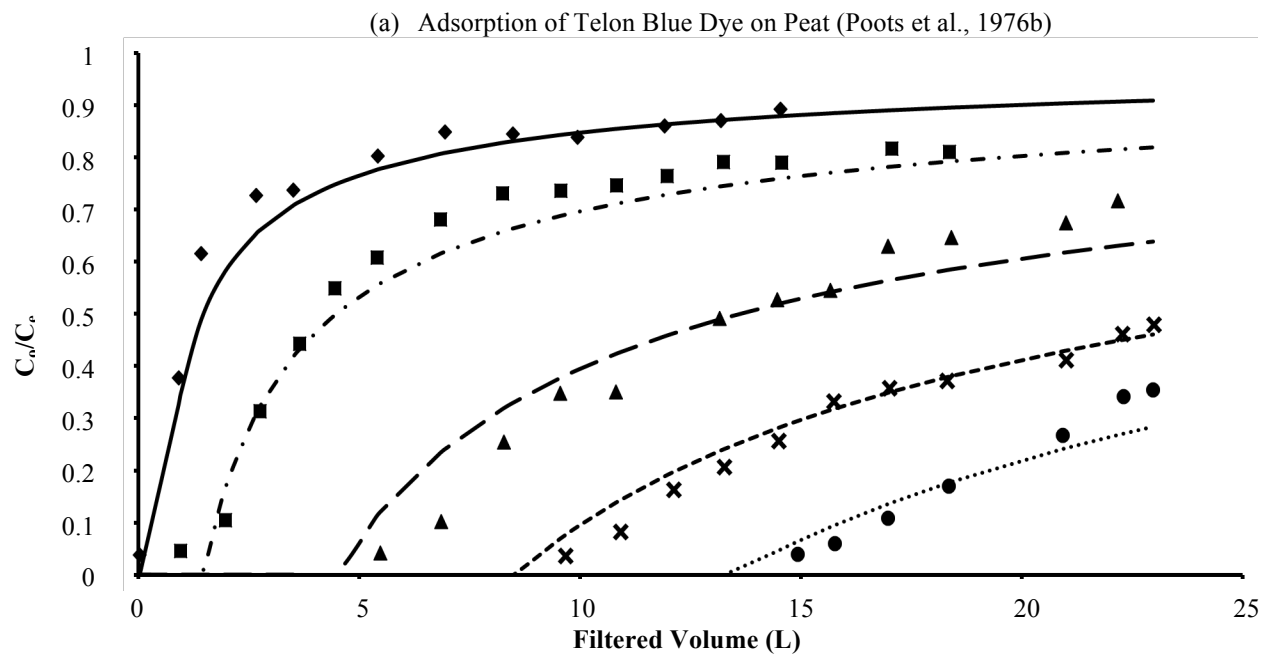


Figure 5

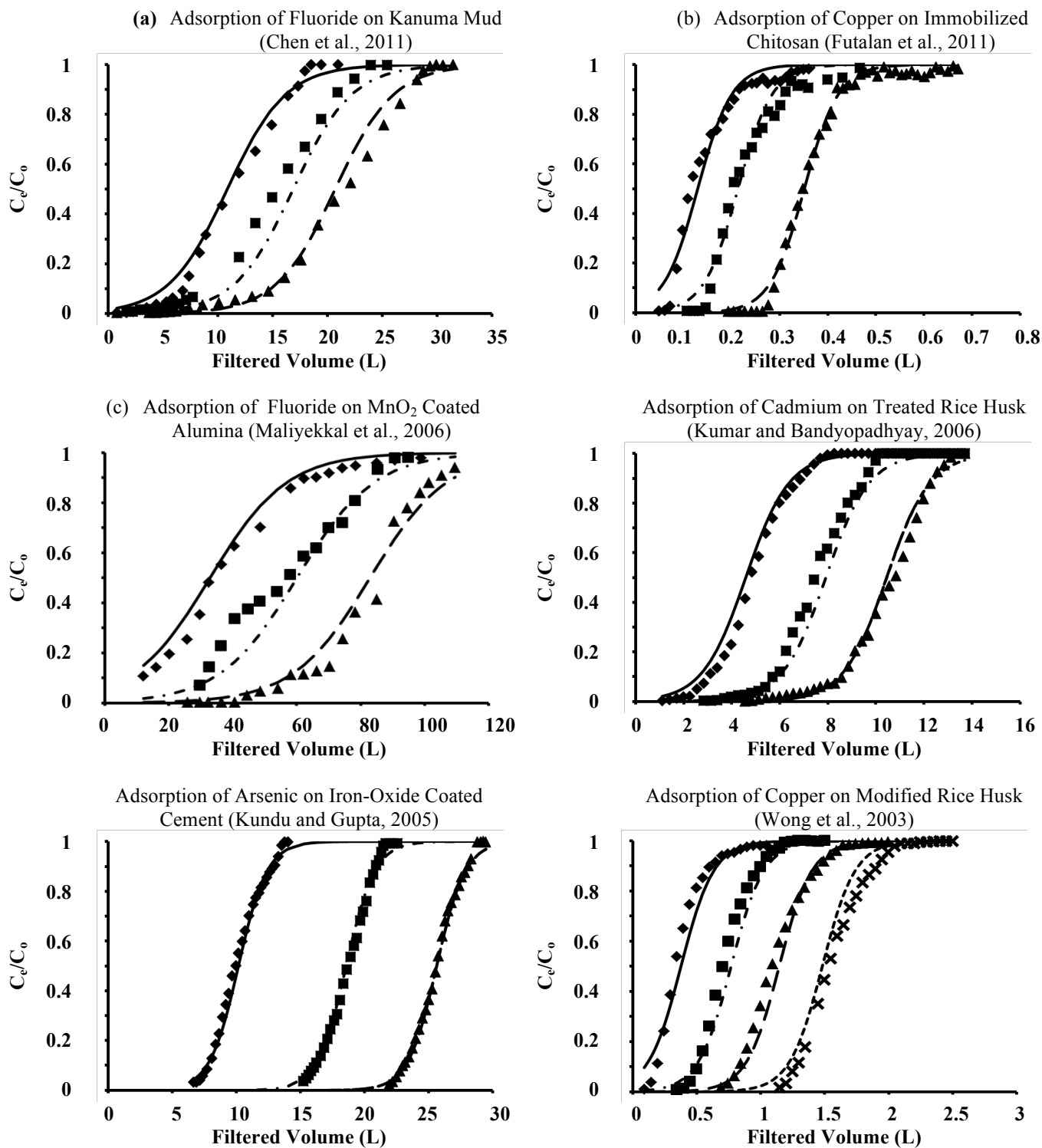
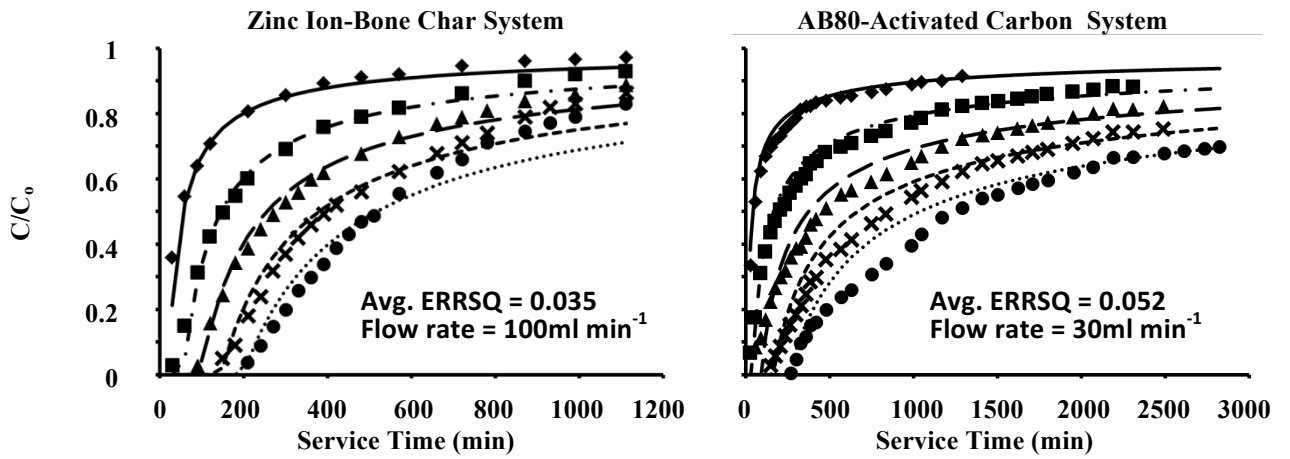


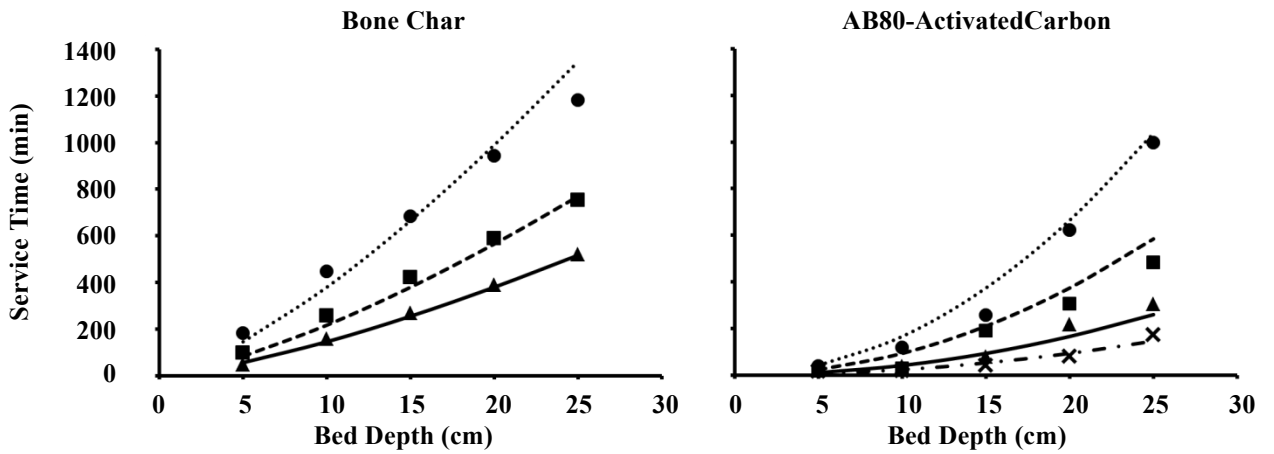
Figure 6 – Data from (Ko et al., 2002)

Breakthrough Curves at Different Bed Depths



Bed Depth: 5cm 10cm 15cm 20cm 25cm
 Experimental: \blacklozenge \blacksquare \blacktriangle \times \bullet
 Model Prediction: — — — — —

Bed Depth Service Time Plots



Flow rate (ml min^{-1}): 50 75 100 30 40 60 80
 Experimental: \bullet \blacksquare \blacktriangle \bullet \blacksquare \blacktriangle \times
 Model Prediction: - - - - -

Table 1.

Equation	Average model ERRSQ values		
	AI-WTR	Fine Conc.	Coarse Conc.
$q_t = q_e(1 - e^{-at})$	0.0762	0.0687	0.0080
$q_t = q_e(1 - e^{-a^*\sqrt{t}})$	1.0534	0.0873	0.1028
$q_t = q_e \frac{t}{t + a^{**}}$	0.0737	0.0568	0.0078

Table 2.

		Model parameters determined from Large Column Data			Model parameters determined from Small Column Data		
		AI-WTR	Coarse Concrete	Fine Concrete	AI-WTR	Coarse Concrete	Fine Concrete
Model Parameters	A	0.0105	0.0062	0.0058	0.0163	0.0071	0.0124
	B	1.2370	1.6385	1.3733	1.3692	1.7606	1.7054
	a**	10.6786	9.1300	1.3525	10.1007	9.2322	1.2134
		Model ERRSQ values			Model ERRSQ values		
		5cm	0.0245	0.0028	0.0038	0.0210	0.0048
Filter Depth	10cm	0.0328	0.0012	0.0027	0.1540	0.0011	0.0282
	18cm	0.0472	0.0032	0.0105	0.0596	0.0034	0.1034
	25cm	0.0209	0.0106	0.0144	0.0291	0.0189	0.0641
	40cm	0.0038	0.0074	0.0228	0.0463	0.0100	0.0735
	μ:	0.0259	0.0050	0.0108	0.0620	0.0076	0.0544